European Journal of Wood and Wood Products (2026) 84:115
https://doi.org/10.1007/s00107-026-02476-4

ORIGINAL ARTICLE

Lignin paradox: selective property enhancement in particleboard

Jozef Martinka[1] · Charalampos Lykidis[2] · Viktor Wallisch[3] · Peter Rantuch[1] · Tomáš Štefko[1] · Igor Wachter[1] · George I. Mantanis[4]

Received: 24 February 2026 / Accepted: 7 August 2026

Abstract

This study investigates how additional lignin powder affects the mechanical performance and fire behaviour of particleboard (PB). Particleboards were manufactured from an industrial wood particle mixture bonded with phenol–formaldehyde (PF) resin (10 wt% constant content) using hot pressing at 7.8 MPa and 210 °C for a total pressing time of 4 min (press time factor was 15 $s \cdot mm^{-1}$). Three board formulations were produced: control boards without lignin addition (PB-0 L), boards containing 10 wt% added lignin powder (PB-10 L), and boards containing 20 wt% added lignin powder (PB-20 L). Fire performance was evaluated using a cone calorimeter under a heat flux of 50 $kW \cdot m^{-2}$. In addition, artificial neural network (ANN) models were developed to predict the carbon monoxide release rate (CORR) and smoke production rate (SPR) based on selected cone calorimeter parameters. The results demonstrate that the incorporation of 20 wt% lignin powder significantly improves fire performance, leading to an almost threefold reduction in total carbon monoxide production, from 735 to 250 $g \cdot m^{-2}$. Simultaneously, the modulus of elasticity increased substantially, from 1855 to 2639 $N \cdot mm^{-2}$. Conversely, the addition of lignin negatively affected the internal bond strength, which decreased from 0.48 to 0.25 $N \cdot mm^{-2}$. The developed ANN models exhibited high predictive accuracy, with normalized root mean square errors below 6% for CORR and approximately 2% for SPR. These findings indicate that lignin powder has strong potential as a sustainable additive for enhancing the fire performance and stiffness of particleboard, although optimization is required to mitigate its adverse effects on internal bonding.

1 Introduction

Agglomerated wood-based products are manufactured from lignocellulosic raw materials (e.g., sawdust, particles, chips, flakes, fibres, strands, or veneers) bonded with synthetic or natural adhesives and consolidated by hot pressing. In some products, surface layers (e.g., laminates or foils) are applied to improve surface resistance, aesthetics, and emission control. The main advantage of agglomerated wood products is the possibility of producing large-format panels from low-value or waste wood resources. The principal categories of such products include particleboard (PB), fibreboard, oriented strandboard, and plywood.

As a versatile wood-based composite, PB has become an essential material in numerous sectors, including construction, furniture manufacturing, interior applications (e.g., wall panelling and decoration), packaging, and flooring (Dukarska et al. 2017; Yang et al. 2024; Long et al. 2026).

The development of sustainable PB production technologies has become increasingly important in response to environmental pressures such as deforestation, waste

✉ Jozef Martinka
jozef.martinka@stuba.sk

✉ Tomáš Štefko
tomas.stefko@stuba.sk

[1] Institute of Integrated Safety, Faculty of Materials Science and Technology in Trnava, Slovak University of Technology in Bratislava, Trnava 91724, Slovakia

[2] School of Forestry and Natural Environment, Laboratory of Wood Technology, Aristotle University of Thessaloniki, Thessaloniki 54124, Greece

[3] Department of Wood Processing and Biomaterials, Czech University of Life Sciences Prague, Kamýcká 129, Prague 165 00, Czech Republic

[4] Department of Forestry, Wood Sciences and Design, Laboratory of Wood Science & Technology, University of Thessaly, Karditsa 43100, Greece

Published online: 17 August 2026

accumulation, and the energy-intensive nature of conventional manufacturing processes. One promising strategy is the incorporation of recycled wood-based materials (e.g., plywood or PB waste) and alternative lignocellulosic resources such as eucalyptus, which contributes to circular material flows and reduces reliance on virgin raw materials (Ranjan et al. 2025). Furthermore, PB can be produced from a wide range of alternative or underutilised materials, either as sole feedstocks or in combination with conventional wood particles. These include, for example, sugar cane bagasse (Bonilla et al. 2015), green coconut waste (Lim et al. 2021), rice husks (Olupot et al. 2022), hemp shives (Papadopoulou et al. 2023), pineapple leaves, recycled extruded polystyrene foam (Cagadas et al. 2023), municipal waste (Lykidis and Grigoriou 2011; Hrušovský and Réh 2024), coconut fibres (Bawono et al. 2025), and various other agricultural residues and industrial by-products (Lykidis et al. 2014).

Wood is a complex lignocellulosic material composed primarily of cellulose (40–55 wt%), hemicelluloses (24–40 wt%), and lignin (18–35 wt%) (Kumar and Sharma 2017a; Haq et al. 2020), together with minor amounts of extractives (approximately 2–10 wt%, occasionally 1–14 wt%) and ash (typically 0.2–1 wt%, occasionally up to ≈5 wt%) (PETTERSEN 1984). The proportions of these components depend on species, growth conditions, sampling location within the tree, and analytical methodology. In addition, the ash content may be artificially increased by the presence of bark in the analysed material.

Many studies (Stamm 1956; Ramiah 1970; Sebio-Puñal et al. 2012; Senneca et al. 2020) have demonstrated that lignin is thermally more stable than cellulose and hemicelluloses under thermal analysis conditions. Moreover, lignin can act as a natural thermoplastic binder during hot pressing of wood-based materials such as particleboards, pellets, and fibreboards, as discussed by Ko et al. (2018), Zhao et al. (2020), and Mili et al. (2022). Phenolic hydroxyl groups in lignin play a crucial role in this binding mechanism (Kai et al. 2016). In addition, lignin exhibits a relatively hydrophobic character, which can contribute to improved water resistance of the final products.

Kraft lignin is a major by-product of the pulp and paper industry (hereafter referred to as technical lignin). This material can be valorised either through material recycling (e.g., in wood-based composites) or through energy recovery. According to the cascade utilisation principle, material use of lignin should be prioritised over its combustion (Sirkin and Houten 1994; Keegan et al. 2013). However, the majority of technical lignin is still used for energy recovery (Ragauskas et al. 2014; Kumar and Sharma 2017b; Dessbesell et al. 2020; Trezza et al. 2025). The application of technical lignin in wood-based composites has therefore attracted increasing research interest. Its use as a partial or complete substitute for synthetic resin binders has been extensively investigated and recently reviewed (Younesi-Kordkheili et al. 2016; Owodunni et al. 2020; Conti Silva et al. 2024; Němec et al. 2024, 2025; Paez and Fatehi 2025). Alternative approaches based on chemical pretreatment of biomass, including in situ lignin polymerisation (Gong et al. 2025) or oxidative cross-linking of natural polymers (Ju et al. 2024), have also been reported. Although these advanced approaches have produced materials with promising properties, their industrial implementation remains limited due to process complexity and cost. Consequently, industrial practice favours simpler and more robust approaches that are compatible with existing large-scale production technologies.

In line with the need for practical industrial applications, several studies have investigated the direct incorporation of lignin, either as a sole binder, a co-adhesive, or a surface treatment, with varying degrees of success. When used as the sole adhesive, unmodified and oxidized lignin powders have historically yielded extremely low internal bond strengths (0 to 0.03 $N \cdot mm^{-2}$) in PBs (Hemmilä et al. 2013). More recent chemical modifications have shown improvement; for instance, Salim et al. (2024) utilized a demethylated bark-lignin gel blended with ammonium chloride, achieving a ≈36% increase in the modulus of elasticity compared to urea-formaldehyde (UF) bonded boards, though internal bond strength remained 20% lower. Blending lignin with existing synthetic resins has proven more stable, as Martínez et al. (2021) demonstrated that the physical and mechanical properties of PBs can be fully maintained up to a 3:1 ratio of Klason lignin to UF resin. Beyond mechanical performance, emerging research has begun to touch upon the fire properties of lignin-enhanced wood products. Shi et al. (2025) reported improvements in both the mechanical and fire properties of poplar wood coated with lignin powder and subsequently hot-pressed. However, their study did not isolate the specific contributions of the lignin powder versus the hot-pressing densification, and the fire performance was limited to a basic flame spread test.

Despite extensive research on lignin as a binder component, its use as a direct particulate additive in particleboard and its influence on fire behaviour, particularly carbon monoxide emissions, remains insufficiently explored. Addressing this gap is essential for improving both the sustainability and fire safety performance of wood-based composites.

Therefore, the aim of this study was to produce particleboards from a mixture of industrial wood particles (derived from construction and carpentry waste), lignin powder (originating from the paper industry), and a commercial phenol–formaldehyde resin using hot pressing. The specific objectives were (i) to evaluate the mechanical and fire performance of these boards, and (ii) to develop and train

Table 1 Properties of the used phenol-formaldehyde resin

Property	Value
pH (–)	11.62
Viscosity at 25 °C	440
Solids content at 2.0 g / 120 °C/ 2 h (wt%)	49
Density (kg·m^{-3})	1240
Alkalinity (wt%)	6.8
Gel time at 0.6 g/ 130 °C (min)	3.5
Molar ratio (-)	1:2.1
Free urea content (wt%)	2

artificial neural network models capable of predicting the carbon monoxide release rate (CORR) and smoke production rate (SPR) based on readily measurable cone calorimeter parameters.

2 Materials and methods

Particleboards (PBs) were manufactured from industrial wood particles (derived from construction and carpentry waste) with a particle size below 8 mm. The furnish consisted of approximately 70% softwoods (predominantly pine *Pinus* spp. and spruce *Picea* spp.) and 30% hardwoods (mainly oak *Quercus* spp. and beech *Fagus* spp.). The particle size distribution comprised four fractions: coarse (8–4 mm, 4.13 ± 0.01 wt%), medium (4–2 mm, 29.18 ± 0,02 wt%), and fine (2–1 mm, 50.64 ± 0.01 wt%) and ultra-fine (< 1 mm, 16.07 ± 0.01 wt%). The material was supplied by AKRITAS S.A. (Alexandroupolis, Greece). Prior to board manufacture, the particles were dried in a laboratory dryer at 60–70 °C to a moisture content of approximately 3 wt%.

Phenol–formaldehyde (PF) resin, supplied by NTL Chemical Consulting S.A. (Thessaloniki, Greece), was used as the adhesive system. The basic properties of the resin are summarised in Table 1. Commercial lignin powder (dealkaline lignin, L0045, CAS RN 8061-51-6) was purchased from Tokyo Chemical Industry Co., Ltd. (Tokyo, Japan). The lignin was supplied as a dry powder with particle sizes ranging from 10 to 100 µm and a pH of 3–4.

2.1 Particleboard preparation

The PF resin was applied to the wood particles in a laboratory rotary drum blender at a rate corresponding to 10 wt% resin solids (based on oven-dry wood mass). The blender operated at approximately 1 Hz and was equipped with an atomiser supplied with compressed air at 0.25 MPa and a resin feed pressure of 0.1 MPa.

Lignin powder was incorporated as a partial substitution for wood particles as a filler (on a dry mass basis) at three levels: 0 wt% (PB-0 L), 10 wt% (PB-10 L), and 20 wt% (PB-20 L), while maintaining a constant PF resin content. The lignin powder was added after resin spraying. For PB-10 L, the lignin was introduced in two equal portions (50:50), each followed by 30 s of mixing. For PB-20 L, the lignin was divided into three equal portions and incorporated in the same manner, with 30 s mixing after each addition. Lignin addition after spraying allowed the tacky resin film on the particle surfaces to improve its distribution and retention. This approach avoided pre-blending lignin into the liquid PF resin, which would increase viscosity and induce premature reaction. Therefore the PF resin content was held constant for PB-OL, PB-10 L, and also for PB-20 L. Consequently, the lignin introduction adds unresinated material that may interrupt the inter-particle bonded network, potentially affecting internal bond strength.

The mat was manually formed in a forming frame of 350 × 300 mm. The mat moisture content was 9–10%, measured using a Precisa HA60 moisture analyser (Precisa Gravimetrics AG, Switzerland). Hot pressing was carried out in a hydraulic press (400 × 400 mm) equipped with heated platens maintained at 210 °C and controlled by proportional–integral–derivative (PID) controllers. Board thickness was controlled using 12.0 mm hardened steel stops. The pressing cycle consisted of three stages: (i) pressure increase to 7.8 MPa within 30 ± 3 s, (ii) pressing at constant pressure (7.8 MPa) for 180 ± 3 s, and (iii) decompression within 30 ± 3 s.

Four panels were produced for each lignin content level, with a target density of 680 kg·m^{-3} at 6.5 wt% water content. The final boards were single-layer PB, of uniform composition through the thickness (no separate face and core layers).

Representative microscopic images of PB-0 L, PB-10 L, and PB-20 L surfaces are shown in Fig. 1. In PB-0 L (Fig. 1a), light regions correspond to wood particles and dark regions to the PF resin matrix. In PB-10 L and PB-20 L

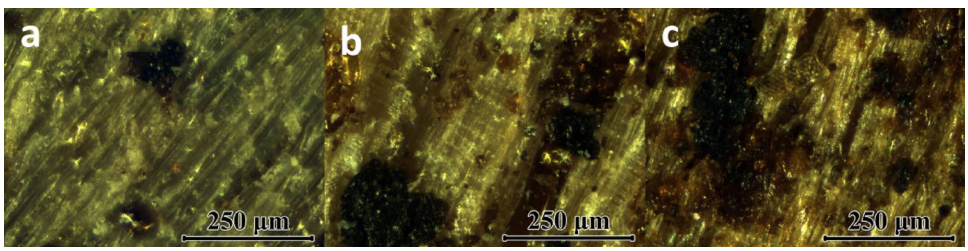

Fig. 1 Microscopic image of investigated PB samples surface: **a** – PB without extra added lignin; **b** – PB with 10 wt% extra added lignin; **c** – PB with 20 wt% extra added lignin

(Fig. 1b, c), the dark phase represents a hybrid matrix consisting of PF resin and lignin formed during hot pressing.

2.2 Mechanical and physical properties

The following properties were determined according to European Standards: density (EN 323:1993), modulus of rupture in static bending (MOR), modulus of elasticity in static bending (MOE) (EN 310: 1993), internal bond strength (IB) (EN 319:1993), thickness swelling (TS), and water absorption (WA) (EN 319:1993).

Prior to testing, specimens were conditioned at 20 ± 0.1 °C and 65 ± 1% relative humidity until constant mass was achieved. Thickness swelling and water absorption were measured after immersion in water for 2, 24, and 48 h.

The statistical significance of the effect of lignin content on mechanical properties was evaluated using the Kruskal–Wallis test (significance level $\alpha = 0.05$), followed by Dunn's post hoc test with Holm–Bonferroni correction, implemented in MATLAB 2025b.

2.3 Thermogravimetric analysis

Thermogravimetric (TG) measurements were performed using a NETZSCH STA 449 F5 Jupiter analyser (Netzsch Gruppe, Selb, Germany). Samples of 10 ± 1 mg were heated from 35 to 650 °C at a heating rate of 10 °C·min^{-1}. Analyses were conducted in two atmospheres: nitrogen (purity 99.9%) and synthetic air (80% N_2 and 20% O_2, both 99.9% purity), with a gas flow rate of 100 mL·min^{-1}.

2.4 Fire performance

Fire performance was evaluated using a dual cone calorimeter (Fire Testing Technology Ltd., East Grinstead, UK) in accordance with ISO 5660-1 (2015). Samples of dimensions (100 × 100 × 12) ± 1 mm were exposed horizontally to an external heat flux of (50 ± 0.5) kW·m^{-2}. Three replicates were tested for each board type.

Prior to testing, samples were dried to constant mass at 103 ± 2 °C and cooled in a desiccator at 23 ± 2 °C. This procedure ensured evaluation under a conservative, low-moisture condition.

The effect size of lignin content on fire performance was evaluated using the absolute value of Cliff's Delta ($|\delta|$) calculated in MATLAB 2025b. Values of $|\delta| \geq 0.474$ were interpreted as a large effect size, following Romano and Kromrey (2006) and Wan et al. (2020).

Table 2 Structure of input data of neural networks for prediction of CO release rate (CORR) and smoke production rate (SPR)

Time (s)	Lignin content (wt%)	SMLR (g·m^{-2}·s^{-1})	HRR (kW·m^{-2})
0 to 1800	0 to 20	0 to 37.5	0 to 375

SMLR specific mass loss rate, *HRR* heat release rate

2.5 Neural network modelling

Artificial neural networks (ANNs) were developed to predict the carbon monoxide release rate (CORR) and smoke production rate (SPR). Four input parameters were used: time from test start, lignin content, specific mass loss rate (SMLR), and heat release rate (HRR). The structure and value ranges of the input data are given in Table 2.

A total of 3249 data records were used, of which 2762 were used for training and 487 for testing. Feedforward neural networks with three layers (4 input neurons, 10 hidden neurons, and 1 output neuron) were implemented using MATLAB 2025b (Deep Learning Toolbox). Bayesian regularisation was used as the training algorithm. The target outputs were CORR (0–0.76 g·m^{-2}·s^{-1}) and SPR (0–7.3 m^2·m^{-2}·s^{-1}).

3 Results and discussion

3.1 Mechanical and physical properties

The mechanical and physical properties of the particleboards are summarised in Table 3. The measured thickness (11.61–11.86 mm), density (676–681 kg·m^{-3}), and equilibrium moisture content (10.8–10.9%) did not differ significantly among PB-0 L, PB-10 L, and PB-20 L, indicating that lignin addition did not result in systematic densification or moisture-related effects. Consequently, the observed differences in performance can be attributed primarily to lignin incorporation.

Lignin addition had a positive effect on bending performance. The modulus of rupture (MOR) increased from 12.01 N·mm^{-2} for PB-0 L to 14.79 N·mm^{-2} for PB-20 L, while PB-10 L showed intermediate values without statistically significant differences from the other groups. A similar trend was observed for the modulus of elasticity (MOE), which increased from 1855 N·mm^{-2} (PB-0 L) to 2639 N·mm^{-2} (PB-20 L), indicating a substantial increase in panel stiffness.

The hygroscopic performance also improved with increasing lignin content. Thickness swelling (TS) and water absorption (WA) after 2, 24, and 48 h immersion were reduced in boards containing lignin, with the most pronounced improvement observed for PB-20 L. These results reflect the hydrophobic nature of lignin and its ability to fill voids within the structure, thereby reducing water uptake and limiting dimensional changes.

Table 3 Mechanical properties and physical properties of PB-0 L, PB-10 L and PB-20 L

Sample	PB-0 L	PB-10 L	PB-20 L
Thickness (mm)	11.86 ± 0.44[a)]	11.79 ± 0.49[a)]	11.61 ± 0.39
Density ($kg \cdot m^{-3}$)	676.08 ± 33.13[a)]	680.80 ± 36.64[a)]	681.33 ± 41.34[a)]
MOR ($N \cdot mm^{-2}$)	12.01 ± 0.90[a)]	12.95 ± 0.88[a)b)]	14.79 ± 1.68[b)]
MOE ($N \cdot mm^{-2}$)	1855 ± 197[a)]	1993 ± 70[a)]	2639 ± 194
IB ($N \cdot mm^{-2}$)	0.48 ± 0.04[a)]	0.44 ± 0.07[a)]	0.25 ± 0.06
TS 2 h (%)	28.25 ± 1.67[a)]	25.39 ± 1.59[a)]	23.19 ± 0.78
TS 24 h (%)	30.48 ± 1.92[a)]	28.24 ± 1.54[a)b)]	27.21 ± 1.26[b)]
TS 48 h (%)	30.72 ± 1.95[a)]	28.76 ± 1.36[a)b)]	28.46 ± 1.57[b)]
WA 2 h (%)	45.87 ± 1.26	42.76 ± 2.21[a)]	41.22 ± 3.01[a)]
WA 24 h (%)	49.46 ± 1.07	46.51 ± 1.89[a)]	45.70 ± 2.39[a)]
WA 48 h (%)	50.84 ± 1.24	48.18 ± 1.91[a)]	47.78 ± 2.35[a)]

MOR modulus of rupture, *MOE* modulus of elasticity, *IB* internal bond strength, *TS* thickness swelling after 2 h to 48 h, *WA* water absorption after 2 h to 48 h, upper indexes [(a)] and [(b)] in the one row indicate data with *p* values of Kruskal-Wallis Dunn's post hoc test higher than 0.05 (no statistically significant difference)

In contrast, internal bond strength (IB) decreased with increasing lignin content. PB-20 L exhibited a significantly lower IB value (0.25 $N \cdot mm^{-2}$) compared with PB-0 L (0.48 $N \cdot mm^{-2}$) and PB-10 L (0.44 $N \cdot mm^{-2}$), while no significant difference was found between PB-0 L and PB-10 L. This reduction can be attributed to the lower reactivity of lignin compared with PF resin and the limited availability of reactive sites for cross-linking reactions (Ghaffar and Fan 2014; Ang et al. 2019; Zhao et al. 2025).

The cause of MOE and MOR increase, while IB decreases with extra incorporated lignin increasing can be explained as follows. MOE and MOR are mainly defined by the stiffness and continuity of the surface layers, where bending stress is highest and where flexural failure begins. During hot pressing the lignin powder softens, fills voids and stiffens the matrix (higher MOE/MOR) and also reduces thickness swelling and water absorption. IB instead exposes the low-density core under perpendicular tension: the extra incorporated lignin physically interrupts the inter-particle PF bonds and introduces a brittle, weakly cohesive phase, so core cohesion (IB) falls. This conclusion is consistent with (Nelis and Mai 2019).

Overall, the results indicate a trade-off between improved stiffness and moisture resistance on one hand and reduced internal bond strength on the other, highlighting the need for optimisation of lignin content and resin formulation.

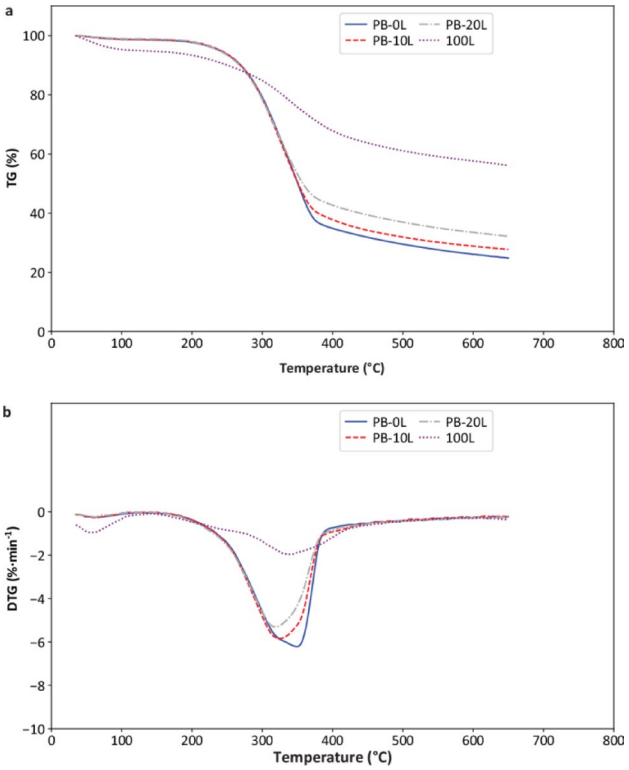

Fig. 2 Thermogravimetric behaviour of particleboards with different lignin contents under nitrogen atmosphere. **a** – TG curves and **b** – DTG curves of particleboards without added lignin (PB-0 L), with 10 wt% lignin (PB-10 L), with 20 wt% lignin (PB-20 L), and pure lignin (100 L), recorded in the temperature range 35–650 °C at a heating rate of 10 °C·min⁻¹

3.2 Thermogravimetric analysis

Thermogravimetric (TG) and derivative thermogravimetric (DTG) curves obtained under inert and oxidative atmospheres are shown in Figs. 2 and 3 and summarised in Table 4.

In nitrogen, two main mass-loss stages were observed. The first stage (approximately 50–150 °C) corresponds to moisture evaporation, while the second stage (approximately 220–400 °C) is associated with the decomposition of hemicelluloses and cellulose (Yang et al. 2007). Lignin degrades over a broader temperature range and contributes to increased char formation. Accordingly, lignin-containing boards exhibited higher residual mass than PB-0 L under inert conditions, confirming the greater thermal stability of lignin.

In oxidative conditions, a third mass-loss stage occurred at approximately 425 °C, corresponding to the heterogeneous oxidation of the remaining char. Despite this oxidation, PB-20 L retained approximately 33% more residue at 650 °C than PB-0 L, demonstrating enhanced char-forming capability.

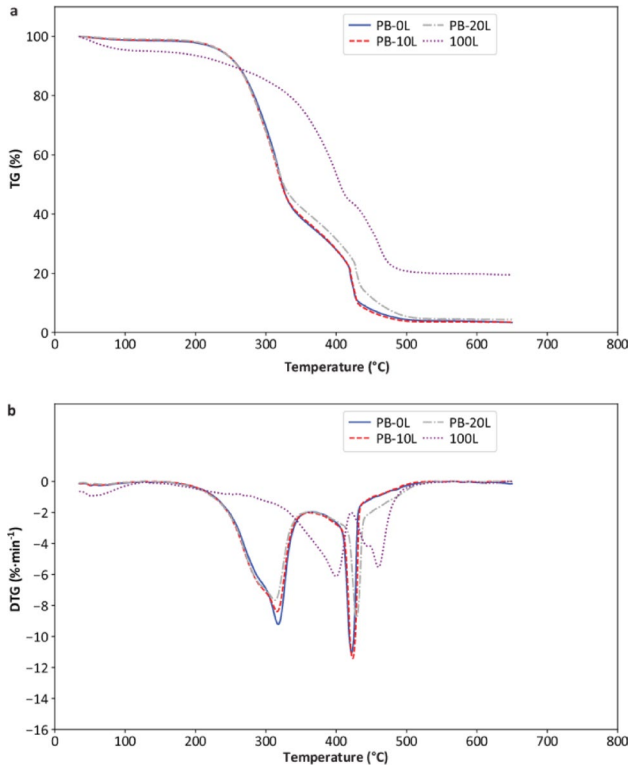

Fig. 3 Thermogravimetric behaviour of particleboards with different lignin contents under oxidative atmosphere (synthetic air). **a** – TG curves and **b** – DTG curves of particleboards without added lignin (PB-0 L), with 10 wt% lignin (PB-10 L), with 20 wt% lignin (PB-20 L), and pure lignin (100 L), recorded in the temperature range 35–650 °C at a heating rate of 10 °C·min^{-1}

These results confirm that lignin incorporation increases char yield and thermal stability, which are important factors influencing fire behaviour.

3.3 Fire performance and combustion behaviour

The time-dependent behaviour of heat release rate (HRR), carbon monoxide release rate (CORR), smoke production rate (SPR), and specific mass loss rate (SMLR) is presented in Fig. 4, with the corresponding time-integrated quantities of total heat release (THR), total CO release (TCOR), total smoke production (TSP), and residual mass (RM), shown as insets. Shaded areas in Figs. 4 and 5 represent standard deviations of the measurements. A comparable influence of lignin incorporation on HRR and SMLR has been reported by (Němec et al. 2025).

At first inspection, the differences among PB-0 L, PB-10 L, and PB-20 L appear relatively small, with the exception of CO-related parameters. The statistical significance of lignin content on the principal fire properties is summarised in Table 5. Notably, TCOR (Fig. 4b inset) shows a substantial and statistically significant reduction for PB-20 L compared with PB-0 L.

The HRR, SPR, and SMLR curves (Fig. 4a, c, d) exhibit similar profiles. An initial peak occurs at ignition, followed by a sharp decline and a second peak. After the second peak, HRR decreases to approximately 60 kW·m^{-2}, while SPR and SMLR approach near-zero values. In contrast, CORR (Fig. 4b) displays a different behaviour, with elevated CO production during the later stage of combustion (approximately 400 s after ignition), corresponding to the formation and oxidation of the char layer.

The second HRR peak is generally attributed to two mechanisms. According to Sanned et al. (2023), it is governed by rear-side boundary conditions, where heat accumulation

Table 4 Thermogravimetric characteristics of particleboards containing 0, 10, and 20 wt% lignin, determined under inert (N_2) and oxidative (80% N_2 + 20% O_2) atmospheres. The first stage corresponds to moisture evaporation, the second stage to devolatilisation of lignocellulosic components, and the third stage (in oxidative atmosphere) to char oxidation

Sample	PB-0 L	PB-10 L	PB-20 L	PB-0 L	PB-10 L	PB-20L
Protective gas	N_2			80% N_2+20% O_2		
1st step						
Temperature range (°C)	50–118	50–148	50–134	50–148	50–136	50–135
Peak temperature(°C)	72	60.1	59.1	63.3	59.3	69.9
Mass loss (%)	1.5	1.4	1.2	1.6	1.5	1.1
2nd step						
Temperature range (°C)	118–750	148–750	136–750	148–366	136–364	135–362
Peak temperature(°C)	348.3	326.2	319.6	318.2	317.1	313.5
Mass loss (%)	73.7	70.9	66.6	62.8	61.6	59.1
3rd step						
Temperature range (°C)	–	–	–	366–650	364–650	362–650
Peak temperature(°C)	–	–	–	422.1	427.4	429.1
Mass loss (%)	–	–	–	32.3	33.5	35.4
Residue at 650 °C (%)	**24.8**	**27.7**	**32.2**	**3.3**	**3.4**	**4.4**

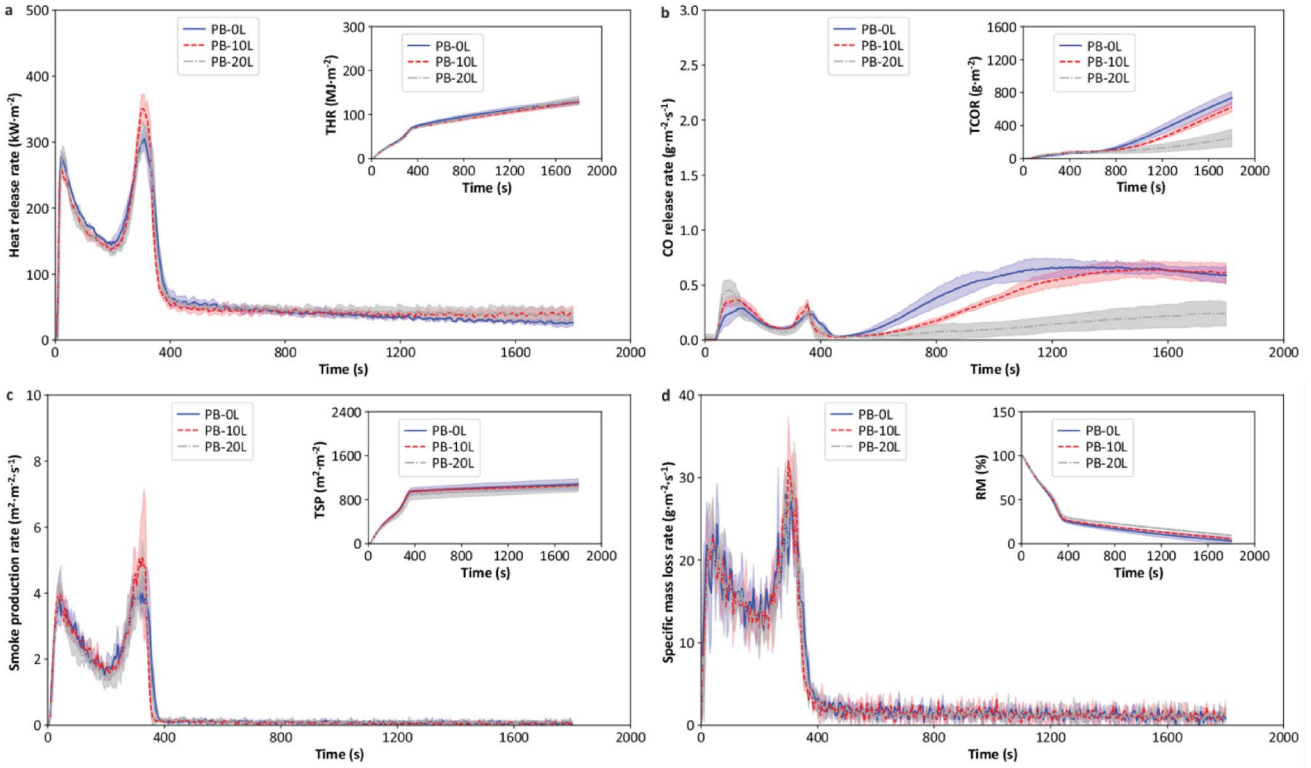

Fig. 4 Time dependencies of **a** – heat release rate and total heat release rate (THR); **b** – CO release rate and total CO release (TCOR); **c** – smoke production rate and total smoke production (TSP); **d** – specific mass loss rate and residual mass (RM) of particle board without extra incorporated lignin (PB-0 L), with 10 wt% extra added lignin (PB-10 L), and with 20 wt% extra incorporated lignin (PB-20 L) (shadow areas around lines indicate standard deviations)

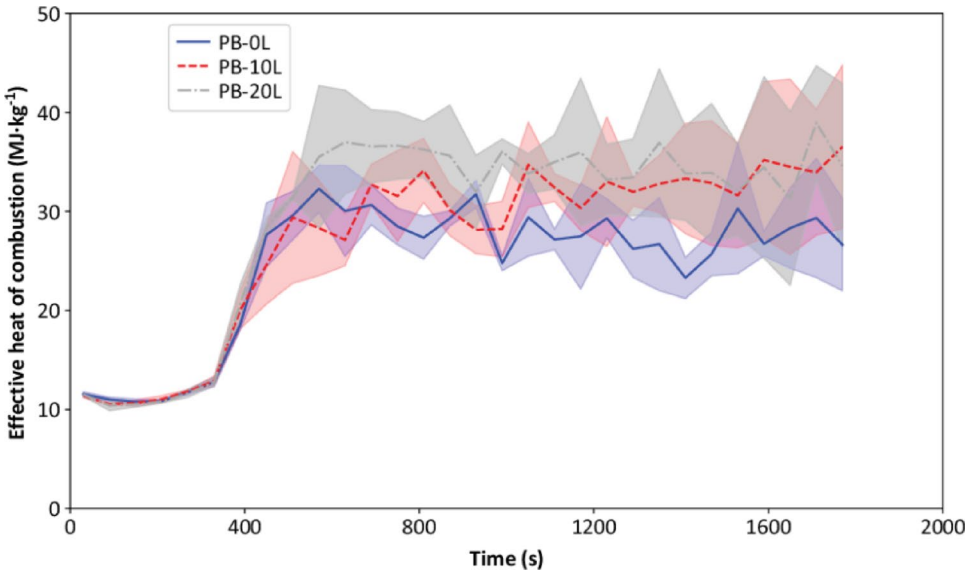

Fig. 5 Time dependence of the effective heat of combustion (EHC) of particleboards with different lignin contents during cone calorimeter testing. Curves correspond to boards without added lignin (PB-0 L), with 10 wt% lignin (PB-10 L), and with 20 wt% lignin (PB-20 L), tested at an external heat flux of 50 kW·m^{-2}

within the sample promotes accelerated pyrolysis. Alternatively, Babrauskas (2023) attributes the second peak to multiple degradation pathways in wood, resulting in different effective heats of combustion during flaming and glowing phases.

The time dependence of effective heat of combustion (EHC) is shown in Fig. 5. Comparison of Figs. 4 and 5 indicates that the decrease of the second HRR peak to approximately 60 kW·m^{-2} at around 400 s corresponds to a stepwise increase in EHC. This increase occurs after the second HRR peak, indicating a transition from flaming to char oxidation.

Table 5 Fire performance parameters of particleboards containing 0, 10, and 20 wt% added lignin determined by cone calorimeter testing at an external heat flux of 50 kW·m⁻². Values are presented as mean ± standard deviation ($n = 3$)

Sample	PB-0 L	PB-10 L	PB-20 L
Time to ignition (s)	9.34 ± 0.58[a)]	9.34 ± 1.15[a)]	13.67 ± 1.53
MARHE (kW·m^{-2})	205.94 ± 5.17	197.86 ± 5.70	192.25 ± 2.44
HRR_{max1} (kW·m^{-2})	277.09 ± 10.15	258.84 ± 8.50	285.04 ± 8.27
Time to HRR_{max1} (s)	20 ± 2	18.34 ± 1.53	30 ± 5
HRR_{max2} (kW·m^{-2})	305.27 ± 19.09	361.01 ± 15.79	317.57 ± 11.62
Time to HRR_{max2} (s)	310 ± 2[a)b)]	308.34 ± 10.41[a)]	317.58 ± 10.41[b)]
THR (MJ·m^{-2})	129.63 ± 5.68[a)]	129.23 ± 6.64[a)]	132.13 ± 9.39[a)]
EHC (MJ·kg^{-1})	15.70 ± 0.64	16.24 ± 0.59	16.77 ± 0.65
Residual mass (%)	3.23 ± 3.80[a)]	5.60 ± 0.52[a)]	9.48 ± 0.63
TCOR (g·m^{-2})	735.55 ± 75.84	624.42 ± 59.78	250.08 ± 102.28
COY per ML (g·kg^{-1})	89.47 ± 7.78	78.32 ± 7.73	32.03 ± 14.09
COY per RH (g·MJ^{-1})	5.69 ± 0.34	4.83 ± 0.954	1.92 ± 0.91
TSP (m^2·m^{-2})	1078.31 ± 101.39[a)]	1054.48 ± 35.71[a)]	1031.38 ± 82.37[a)]
SEA per ML (m^2·kg^{-1})	131.44 ± 7.92[a)]	132.58 ± 2.75[a)]	131.35 ± 14.53[a)]
SEA per RH (m^2·MJ^{-1})	8.37 ± 0.44[a)]	8.17 ± 0.18[a)]	7.86 ± 1.15[a)]

MARHE maximum average rate of heat emission, *HRR_{max1} and HRR_{max2}* first and second peak values of heat release rates during the cone calorimeter test, respectively, *THR and EHC* total heat release and effective heat of combustion respectively, *TCOR* total CO release, *COY per ML and COY per RH* carbon monoxide yield per mass loss of sample or per unit of released heat, respectively, *TSP* total smoke production, *SEA per ML and SEA per RH* smoke extinction area per mass loss of sample or per unit of released heat, respectively, upper indexes

[a)] and [b)] in one row indicate data with Cliff's Delta (|δ|) absolute value of |δ| < 0.474, which corresponds to a negligible effect size according to Romano and Kromrey (2006) and Wan et al. (2020)

Average EHC values for three time intervals (0–330 s, 330–510 s, and 510–1800 s) are summarised in Table 6. Statistical analysis (Kruskal–Wallis test with Dunn's post hoc comparisons) shows that lignin addition does not significantly affect EHC during the active flaming phase

Table 6 Effective heat of combustion (EHC) of PB with 0 to 20 wt% extra incorporated powder lignin at the three time intervals

Time interval (s)	EHC (MJ·kg^{-1})		
	Extra incorporated lignin (wt%)		
	0	10	20
0 to 330	11.46 ± 0.75[a)]	11.40 ± 0.86[a)]	11.28 ± 0.90[a)]
330 to 510	22.15 ± 7.32[b)]	21.74 ± 7.19[b)]	23.33 ± 7.61[b)]
510 to 1800	28.21 ± 3.57	31.95 ± 4.85	34.75 ± 4.93

Upper indexes [a)] and [b)] indicate data with p values of Kruskal-Wallis Dunn's post hoc test higher than 0.05 (statistical no significant difference)

(HRR > 50 kW·m^{-2}) but leads to a significant increase during the charring phase. This behaviour is consistent with results reported by (Todaro et al. 2015, 2020), who reported increased calorific value in lignin-rich materials.

The correspondence between HRR, SPR, and SMLR behaviour suggests that the second peak observed in SPR and SMLR originates from the same thermophysical mechanism as the second HRR peak, as proposed by Sanned et al. (2023).

Overall, the incorporation of lignin has only a moderate effect on most fire performance parameters (Table 5). However, a pronounced and statistically significant reduction in all CO-related parameters is observed. The residual mass increases from approximately 3.2 wt% for PB-0 L to approximately 9.5 wt% for PB-20 L, which is relevant for improved fire resistance. In addition, the EHC increases by approximately 6%, which may be beneficial from an energy recovery perspective. The most notable finding is the substantial reduction in CO emissions, which warrants further mechanistic interpretation.

The HRR values of the investigated particleboards are comparable to those reported for fibreboards treated with fire retardants by Mantanis et al. (2020), indicating that lignin addition does not adversely affect the heat release characteristics of the material. In contrast, the CO yield of PB-0 L (approximately 90 g·kg^{-1}) is substantially higher than that reported for solid spruce wood (approximately 30 g·kg^{-1}) by Martinka et al. (2014). The incorporation of 20 wt% lignin reduces the CO yield to values comparable with solid wood, demonstrating a marked improvement in combustion efficiency and fire safety performance.

Incomplete combustion produces soot and partially oxidised gaseous species, primarily CO. Because soot formation correlates with SPR (Östman 2009), trends in CO and SPR provide an indication of combustion efficiency. Visual analysis of Fig. 4 shows that PB-10 L and PB-20 L exhibit slightly higher initial CORR peaks and somewhat elevated second SPR peaks compared with PB-0 L; however, these differences have little influence on total emissions.

The most important observation is that the phase of substantially reduced CORR for lignin-containing boards

begins at approximately 600 s (Fig. 4b), corresponding to the glowing phase of char oxidation. This indicates that lignin primarily influences CO generation during the char oxidation stage rather than during flaming combustion.

The reduction in CO emissions is therefore likely associated with the properties of the lignin-derived char layer. Lignin pyrolysis produces a higher yield of phenolic compounds and hydroxyl functional groups (Jiang et al. 2010; Zhang et al. 2023), which may promote oxidation of CO to CO_2 (Moulijn and Kapteijn 1995). In addition, lignin forms a denser and less porous char than cellulose-derived material (Moulijn and Kapteijn 1995; Sharma et al. 2004; Yang et al. 2007; Xiang et al. 2025). This results in a thicker and more compact char layer that restricts oxygen diffusion to the underlying material, thereby modifying the combustion regime.

These combined chemical and structural effects are considered to be the primary reasons for the observed reduction in TCOR and CO yield in lignin-containing particleboards.

Comprehensive comparison of the effect of extra incorporated lignin on mechanical and physical properties, thermal analysis, and fire performance indicates adding 10 wt% of lignin is more beneficial than 20 wt% of lignin. An exception may be the need to significantly reduce the carbon monoxide yield, when the addition of 20 wt% lignin is very advantageous.

3.4 Neural network prediction of CORR and SPR

The predictive performance of the developed artificial neural networks (ANNs) for carbon monoxide release rate (CORR) and smoke production rate (SPR) is summarised in Tables 7 and 8 and illustrated in Fig. 6.

The ANN models achieved high predictive accuracy for both target variables. For CORR prediction, the coefficient of determination (R^2) reached 0.962 in the testing phase, with a normalised root mean square error (NRMSE) below 6%. Similarly, for SPR prediction, the testing-phase R^2 exceeded 0.97, while the NRMSE was approximately 2%. These results indicate strong agreement between predicted and measured values across the full range of experimental conditions.

The model performance is further supported by low mean square error (MSE) and root mean square error (RMSE) values, as well as acceptable coefficients of variation of RMSE. The consistency between training and testing datasets confirms that the models do not suffer from significant overfitting and exhibit good generalisation capability.

Comparison with previously published machine-learning approaches in fire engineering and wood science (Yuen et al. 2006; Kopúnek et al. 2024; Zhang et al. 2025; Mozafari Parsa and Tahsini 2025) demonstrates that the present ANN models achieve comparable or superior predictive accuracy. This confirms that reliable prediction of CORR and SPR can be achieved using a limited set of readily measurable input parameters, namely time, lignin content, heat release rate, and specific mass loss rate.

Table 7 Performance metrics of the artificial neural network model for prediction of carbon monoxide release rate (CORR) during training and testing phases

Parameter	Training	Testing
MSE ($g \cdot m^{-2} \cdot s^{-1}$)	0.0017	0.0020
RMSE ($g \cdot m^{-2} \cdot s^{-1}$)	0.0412	0.0447
R^2 (-)	0.9688	0.9621
NRMSE (%)	5.42	5.89
CV(RMSE) (%)	13.86	15.03

MSE mean squared error, *RMSE* root mean square error, R^2 coefficient of determination, *NRMSE* normalized mean square error, *CV(RMSE)* coefficient of variation of root mean square error

Table 8 Performance metrics of the artificial neural network model for prediction of smoke production rate (SPR) during training and testing phases

Parameter	Training	Testing
MSE ($m^2 \cdot m^{-2} \cdot s^{-1}$)	0.0264	0.0250
RMSE ($m^2 \cdot m^{-2} \cdot s^{-1}$)	0.1625	0.1581
R^2 (-)	0.9782	0.9793
NRMSE (%)	2.23	2.17
CV(RMSE) (%)	27.78	27.02

MSE mean squared error, *RMSE* root mean square error, R^2: coefficient of determination, *NRMSE* normalized mean square error, *CV(RMSE)* coefficient of variation of root mean square error

The trained neural network models are provided in the Supplementary information (Supplementary Information A for CORR prediction and Supplementary Information B for SPR prediction). These models can be directly implemented for prediction of CO and smoke emission behaviour of particleboards based on experimentally accessible cone calorimeter data, facilitating their use in fire safety engineering and material development.

4 Conclusion

PBs were manufactured from industrial wood particles, PF resin, and extra incorporated technical dealkaline lignin powder at three different contents: 0, 10, and 20 wt%.

Obtained results prove that 10 wt% extra incorporated lignin maintain or slightly improve most of mechanical, physical, and fire performance properties of PBs. Waste dealkaline lignin at 10 wt% is therefore suitable for recovery as filler in the production of PBs.

On the other hand, 20 wt% extra incorporated lignin significantly improve most of mechanical, physical, and fire performance properties, e.g. MOR, MOE, TS, WA, MARHE, residual mass, and carbon monoxide yield. Other

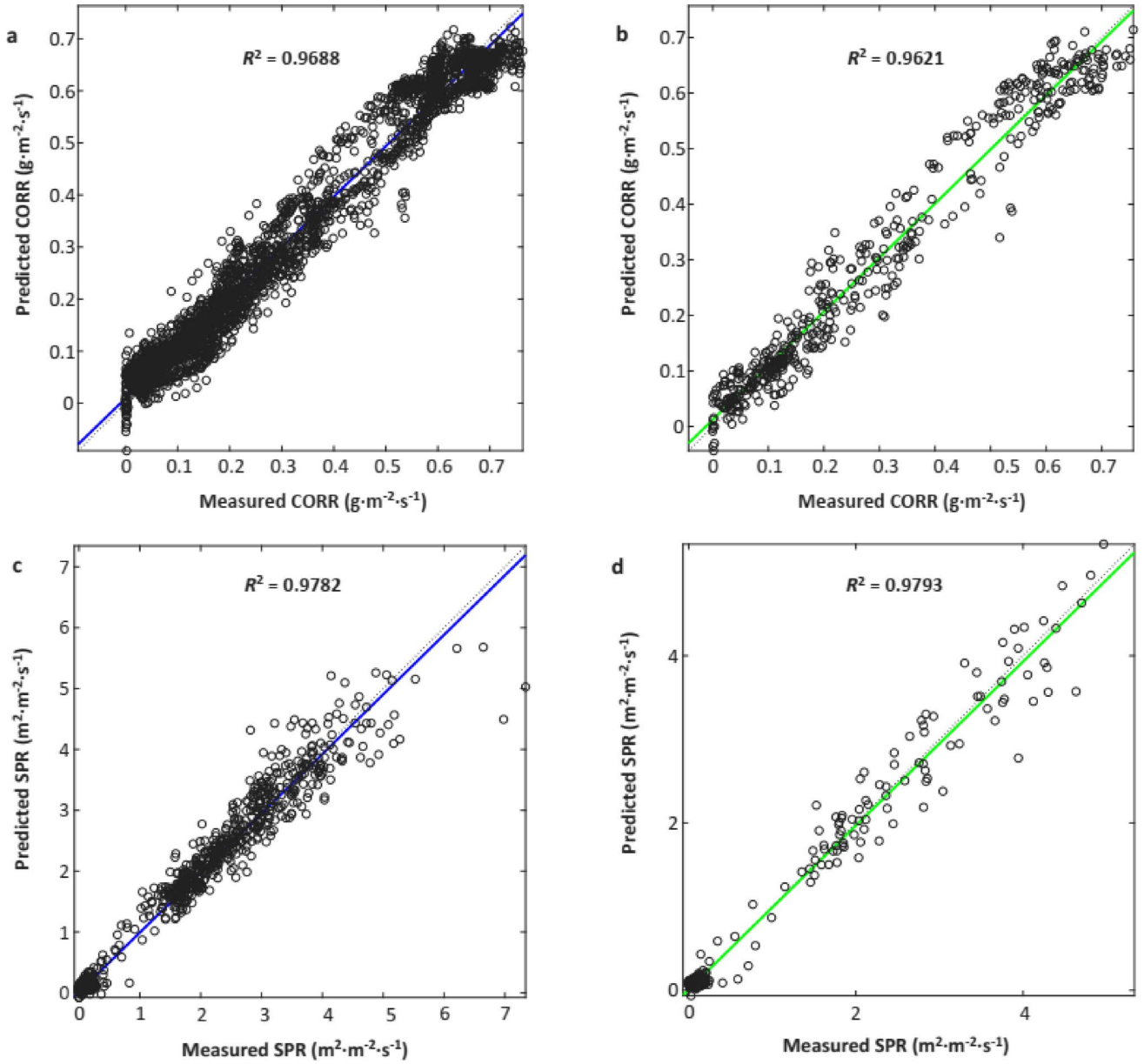

Fig. 6 Comparison of predicted and measured values obtained from the neural network models: **a** – CORR during training phase, **b** – CORR during testing phase, **c** – SPR during training phase, and **d** – SPR during testing phase

fire properties were maintained or only slightly (practically insignificant) deteriorated. The key problem remains IB reduction from 0.48 N·mm^{-2} to 0.25 N·mm^{-2}. Therefore the role of lignin at 20 wt% appears paradoxical. While most properties improved, IB deteriorated significantly. Future research should focus on improving IB at 20 wt% lignin content. Solving this problem would enable lignin to become a high-performance, eco-friendly CO suppressant.

In addition to the experimental work, artificial neural network models were developed to predict carbon monoxide release rate (CORR) and smoke production rate (SPR) from readily measurable cone calorimeter parameters. The trained models achieved high predictive accuracy, with normalised root mean square errors of approximately 6% for CORR and 2% for SPR.

Supplementary Information The online version contains supplementary material available at https://doi.org/10.1007/s00107-026-02476-4.

Acknowledgements This work was supported by the Slovak Research and Development Agency under the Contract no. APVV-24-0143. This work was also supported by the VEGA agency for the project VEGA 1/0755/25.

Author contributions J.M. conceived the study and the concept of

lignin incorporation, developed and trained the artificial neural network models, performed simulations, and contributed to manuscript preparation. C.L. and V.W. prepared the particleboards, carried out mechanical and hygroscopic testing, and drafted the initial version of the manuscript. P.R. conducted the fire performance experiments and performed an evaluation of the fire test data. I.W. and T.Š. performed data analysis and prepared the final version of the manuscript. G.I.M. supervised the project, contributed to the overall study design, and critically revised the manuscript. All authors reviewed and approved the final manuscript.

Funding This work was supported by the Slovak Research and Development Agency under the Contract no. APVV-24-0143. This work was also supported by the VEGA agency for the project VEGA 1/0755/25.
Data availability.
Data will be made available on request.

Data availability All data supporting the findings of this study are available within the paper and its Supplementary Information. The trained neural network models are provided in the Supplementary information (Supplementary Information A for CORR prediction and Supplementary Information B for SPR prediction).

Declarations

Conflict of interests The authors declare no competing interests.

References

Ang AF, Ashaari Z, Lee SH et al (2019) Lignin-based copolymer adhesives for composite wood panels – A review. Int J Adhes Adhes 95:102408. https://doi.org/10.1016/j.ijadhadh.2019.102408

Babrauskas V (2023) Comments on The curious case of the second/end peak in the heat release rate of wood: A cone calorimeter investigation, by Sanned et al. Fire Mater 47:733–734. https://doi.org/10.1002/fam.3143

Bawono NMH, Bawono B, Anggoro PW, Jamari J (2025) Study of application of coconut coir fiber-based wood-based panels: A literature review. Compos Part C Open Access 17:100588. https://doi.org/10.1016/j.jcomc.2025.100588

Bonilla S, Marmol G, Fiorelli J, Savastano H Jr (2015) Particleboard with coir fiber and sugar cane bagasse: thermal-physical-mechanical properties. Acad J Civ Eng 33:682–686. https://doi.org/10.26168/icbbm2015.106

Cagadas ZRB, Barcelona KF, Tadena WF et al (2023) Properties of particleboard made from waste pineapple leaves and recycled styrofoam. Sci Int(Lahore) 35:739–743

Conti Silva JA, Patel P, Pazymino I et al (2024) Effective Lignin-Based Binders for Particle Boards. ACS Sustain Resour Manag 1:1225–1237. https://doi.org/10.1021/acssusresmgt.4c00088

Dessbesell L, Paleologou M, Leitch M et al (2020) Global lignin supply overview and kraft lignin potential as an alternative for petroleum-based polymers. Renew Sustain Energy Rev 123:109768. https://doi.org/10.1016/j.rser.2020.109768

Dukarska D, Czarnecki R, Dziurka D, Mirski R (2017) Construction particleboards made from rapeseed straw glued with hybrid pMDI/PF resin. Eur J Wood Wood Prod 75:175–184. https://doi.org/10.1007/s00107-016-1143-x

European Committee for Standardization (1993a) EN 323:1993 Wood-based panels. - Determination of density

European Committee for Standardization (1993b) EN 310:1993 Wood-based panels -. Determination of modulus of elasticity in bending and of bending strength

European Committee for Standardization (1993c) EN 319:1993 Particleboards and fibreboards - Determination of tensile strength perpendicular to the plane of the board

European Committee for Standardization (1993d) EN 317:1993 Particleboards and fibreboards - Determination of swelling in thickness after immersion in water

Ghaffar SH, Fan M (2014) Lignin in straw and its applications as an adhesive. Int J Adhes Adhes 48:92–101. https://doi.org/10.1016/j.ijadhadh.2013.09.001

Gong Z, Yang G, Chen L, Shuai L (2025) Self-adhesion lignin bonding for the production of particleboards from low-grade wood. Environ Chem Lett 23:1171–1176. https://doi.org/10.1007/s10311-025-01835-6

Haq I, Mazumder P, Kalamdhad AS (2020) Recent advances in removal of lignin from paper industry wastewater and its industrial applications – A review. Bioresour Technol 312:123636. https://doi.org/10.1016/j.biortech.2020.123636

Hemmilä V, Trischler J, Sandberg D (2013) Lignin: an adhesive raw material of the future or waste of research energy? In: Northern European Network for Wood Science and Engineering (WSE. Proceedings of the 9th meeting, September 11–12, 2013, Hannover, Germany. Leibniz Universität, pp 98–103

Hrušovský D, Réh R (2024) Properties of particleboard made from recycled municipal waste and wood particles. Acta Fac Xylologiae Zvolen 66:33–46

International Organization for Standardization (2015) Reaction-to-fire tests — Heat release, smoke production and mass loss rate Part 1: Heat release rate (cone calorimeter method) and smoke production rate (dynamic measurement). Geneva, Switzerland

Jiang G, Nowakowski DJ, Bridgwater AV (2010) Effect of the Temperature on the Composition of Lignin Pyrolysis Products. Energy Fuels 24:4470–4475. https://doi.org/10.1021/ef100363c

Ju T, Liu L, Jiang Y et al (2024) High-Performance, Adhesive-Free, Sustainable Biomass-Based Materials Via a Selective in Situ Oxidation Interface. ACS Sustain Chem Eng 12:13316–13325. https://doi.org/10.1021/acssuschemeng.4c05157

Kai D, Tan MJ, Chee PL et al (2016) Towards lignin-based functional materials in a sustainable world. Green Chem 18:1175–1200. https://doi.org/10.1039/C5GC02616D

Keegan D, Kretschmer B, Elbersen B, Panoutsou C (2013) Cascading use: a systematic approach to biomass beyond the energy sector. Biofuels Bioprod Biorefining 7:193–206. https://doi.org/10.1002/bbb.1351

Ko H, Zhai L, Park JH et al (2018) Poly(vinyl alcohol)–lignin blended resin for cellulose-based composites. J Appl Polym Sci 135:46655. https://doi.org/10.1002/app.46655

Kopúnek J, Martinka J, Rantuch P et al (2024) Preliminary study of dependence of smoke and carbon monoxide emission on heat release rate from fast-growing wood species. Wood Res 69:222–236. https://doi.org/10.37763/wr.1336-4561/69.2.222236

Kumar AK, Sharma S (2017a) Recent updates on different methods of pretreatment of lignocellulosic feedstocks: a review. Bioresour Bioprocess 4:7. https://doi.org/10.1186/s40643-017-0137-9

Kumar AK, Sharma S (2017b) Recent updates on different methods of pretreatment of lignocellulosic feedstocks: a review. Bioresour Bioprocess 4:7. https://doi.org/10.1186/s40643-017-0137-9

Lim JX, Ong TK, Ng CK et al (2021) Development of Particleboard from Green Coconut Waste. J Phys Conf Ser 2120:012034. https://doi.org/10.1088/1742-6596/2120/1/012034

Long K, Lu W, Pan X et al (2026) Investigation of bonding interface structure-property relationships in particleboard using fluorescence microscopy and digital image correlation. Eur J Wood Prod 84:17. https://doi.org/10.1007/s00107-025-02353-6

Lykidis C, Grigoriou A (2011) Quality characteristics of hydrothermally recycled particleboards using various wood recovery parameters. Int Wood Prod J 2:38–43. https://doi.org/10.1179/2042645311Y.0000000002

Lykidis C, Grigoriou A, Barboutis I (2014) Utilisation of wood biomass residues from fruit tree branches, evergreen hardwood shrubs and Greek fir wood as raw materials for particleboard production. Part A. Mechanical properties. Wood Mater Sci Eng 9:202–208. https://doi.org/10.1080/17480272.2013.875589

Mantanis GI, Martinka J, Lykidis C, Ševčík L (2020) Technological properties and fire performance of medium density fibreboard (MDF) treated with selected polyphosphate-based fire retardants. Wood Mater Sci Eng 15:303–311. https://doi.org/10.1080/17480272.2019.1596159

Martínez J, Jaramillo N, Álvarez C et al (2021) Effect of the addition of lignin on the physical-mechanical properties of particleboards made with pine/ hydrangea stems. Int Wood Prod J 13:1–6. https://doi.org/10.1080/20426445.2021.1998301

Martinka J, Hroncová E, Chrebet T, Balog K (2014) The influence of spruce wood heat treatment on its thermal stability and burning process. Eur J Wood Prod 72:477–486. https://doi.org/10.1007/s00107-014-0805-9

Mili M, Hashmi SAR, Ather M et al (2022) Novel lignin as < scp>natural-biodegradable binder for various sectors—A review. J Appl Polym Sci 139:51951. https://doi.org/10.1002/app.51951

Moulijn JA, Kapteijn F (1995) Towards a unified theory of reactions of carbon with oxygen-containing molecules. Carbon N Y 33:1155–1165. https://doi.org/10.1016/0008-6223(95)00070-T

Mozafari Parsa MM, Tahsini AM (2025) Predicting the transient burning of non-charring materials using physics-informed neural networks. Fire Saf J 153:104379. https://doi.org/10.1016/j.firesaf.2025.104379

Němec M, Prokůpek L, Obst V et al (2024) Novel kraft-lignin-based adhesives for the production of particleboards. Compos Struct 344:118344. https://doi.org/10.1016/j.compstruct.2024.118344

Němec M, Janesch J, Sahula L et al (2025) Development of an innovative powder adhesive based on epoxy-polyester and lignin for production of particleboards. Case Stud Constr Mater 23:e04985. https://doi.org/10.1016/j.cscm.2025.e04985

Nelis PA, Mai C (2019) Improved strength properties of three-layered particleboards with different core and surface layers based on kiri wood (Paulownia spp). Eur J Wood Prod 77:761–769. https://doi.org/10.1007/s00107-019-01442-7

Östman BA-L (2009) Smoke and Soot. In: Babrauskas V, Grayson SJ (eds) Heat Release in Fires, 2nd edn. Interscience communications, London

Olupot PW, Menya E, Lubwama F et al (2022) Effects of sawdust and adhesive type on the properties of rice husk particleboards. Results Eng 16:100775. https://doi.org/10.1016/j.rineng.2022.100775

Owodunni AA, Lamaming J, Hashim R et al (2020) Adhesive application on particleboard from natural fibers: A review. Polym Compos 41:4448–4460. https://doi.org/10.1002/pc.25749

Paez J, Fatehi P (2025) Incorporation of lignin into adhesives: a review. Green Chem 27:12499–12537. https://doi.org/10.1039/D5GC02998H

Papadopoulou E, Chrysafi I, Karidi K et al (2023) Particleboards with Recycled Material from Hemp-Based Panels. Mater (Basel) 17:139. https://doi.org/10.3390/ma17010139

PETTERSEN RC (1984) The Chemical Composition of Wood. The Chemistry of Solid Wood. American Chemical Society, pp 57–126

Ragauskas AJ, Beckham GT, Biddy MJ et al (2014) Lignin Valorization: Improving Lignin Processing in the Biorefinery. Sci (80-) 344:1246843. https://doi.org/10.1126/science.1246843

Ramiah MV (1970) Thermogravimetric and differential thermal analysis of cellulose, hemicellulose, and lignin. J Appl Polym Sci 14:1323–1337. https://doi.org/10.1002/app.1970.070140518

Ranjan M, Murali G, Mamatha BS et al (2025) Sustainable alternatives in particleboard production: The role of leveraging recycled and renewable materials. Results Eng 27:106020. https://doi.org/10.1016/j.rineng.2025.106020

Romano J, Kromrey J, Coraggio J, Skowronek J (2006) Appropriate Statistics for Ordinal Level Data: Should We Really Be Using t-test and Cohen's d for Evaluating Group Differences on the NSSE and other Surveys? In: Annual meeting of the Florida Association of Institutional Research. Cocoa Beach, Florida

Salim RM, Asik J, Sarjadi MS (2024) Properties of Bark Particleboard Bonded with Demethylated Lignin Adhesives Derived from Leucaena leucocephala Bark. J Renew Mater 12:737–769. https://doi.org/10.32604/jrm.2024.045695

Sanned E, Mensah RA, Försth M, Das O (2023) The curious case of the second/end peak in the heat release rate of wood: A cone calorimeter investigation. Fire Mater 47:498–513. https://doi.org/10.1002/fam.3122

Sebio-Puñal T, Naya S, López-Beceiro J et al (2012) Thermogravimetric analysis of wood, holocellulose, and lignin from five wood species. J Therm Anal Calorim 109:1163–1167. https://doi.org/10.1007/s10973-011-2133-1

Senneca O, Cerciello F, Russo C et al (2020) Thermal treatment of lignin, cellulose and hemicellulose in nitrogen and carbon dioxide. Fuel 271:117656. https://doi.org/10.1016/j.fuel.2020.117656

Sharma RK, Wooten JB, Baliga VL et al (2004) Characterization of chars from pyrolysis of lignin. Fuel 83:1469–1482. https://doi.org/10.1016/j.fuel.2003.11.015

Shi Y, Cai Y, Jiang J et al (2025) Recycling Waste Lignin as Natural Adhesive to Prepare Sustainable. Wooden Compos Mater Eco-Mat 7:e70024. https://doi.org/10.1002/eom2.70024

Sirkin T, ten Houten M (1994) The cascade chain. Resour Conserv Recycl 10:213–276. https://doi.org/10.1016/0921-3449(94)90016-7

Stamm AJ (1956) Thermal Degradation of Wood and Cellulose. Ind Eng Chem 48:413–417. https://doi.org/10.1021/ie51398a022

Todaro L, Rita A, Cetera P, D'Auria M (2015) Thermal treatment modifies the calorific value and ash content in some wood species. Fuel 140:1–3. https://doi.org/10.1016/j.fuel.2014.09.060

Todaro L, Cetera P, Lo Giudice V et al (2020) High calorific value of lignin derived from turkey oak wood: combined effect of steaming and thermal treatment. In: 28th European Biomass Conference and Exhibition. pp 616–617

Trezza A, Mahboob L, Visibelli A et al (2025) Lignin Waste Valorization in the Bioeconomy Era: Toward Sustainable Innovation and Climate Resilience. Appl Sci 15:8038. https://doi.org/10.3390/app15148038

Wan Z, Xia X, Lo D, Murphy GC (2020) How does Machine Learning Change Software Development Practices? IEEE Trans Softw Eng 47:1–1. https://doi.org/10.1109/TSE.2019.2937083

Xiang A, Ebdon JR, Kandola BK (2025) Mechanistic study of char formation in lignin and a lignin/biopolyamide blend for value-added

applications. Ind Crops Prod 233:121361. https://doi.org/10.1016/j.indcrop.2025.121361

Yang H, Yan R, Chen H et al (2007) Characteristics of hemicellulose, cellulose and lignin pyrolysis. Fuel 86:1781–1788. https://doi.org/10.1016/j.fuel.2006.12.013

Yang S, Li M, Wang Y et al (2024) Industrial-scale manufacturing of particleboards using agricultural waste camellia oleifera shells. Constr Build Mater 424:135922. https://doi.org/10.1016/j.conbuildmat.2024.135922

Younesi-Kordkheili H, Pizzi A, Niyatzade G (2016) Reduction of Formaldehyde Emission from Particleboard by Phenolated Kraft Lignin. J Adhes 92:485–497. https://doi.org/10.1080/00218464.2015.1046596

Yuen RKK, Lee EWM, Lo SM, Yeoh GH (2006) Prediction of temperature and velocity profiles in a single compartment fire by an improved neural network analysis. Fire Saf J 41:478–485. https://doi.org/10.1016/j.firesaf.2006.03.003

Zhang Y, Stepanova S, Van Aelst K, Sels BF (2023) Consider lignin's hydroxyl groups content and type, its molecular weight and content when converting it into epoxy resin. Curr Opin Green Sustain Chem 40:100750. https://doi.org/10.1016/j.cogsc.2022.100750

Zhang Z, Zhong H, Avramidis S et al (2025) Transfer learning for predicting wood density of different tree species: calibration transfer from portable NIR spectrometer to hyperspectral imaging. Wood Sci Technol 59:19. https://doi.org/10.1007/s00226-024-01615-5

Zhao Y, Yue J, Tao L et al (2020) Effect of lignin on the self-bonding of a natural fiber material in a hydrothermal environment: Lignin structure and characterization. Int J Biol Macromol 158:1135–1140. https://doi.org/10.1016/j.ijbiomac.2020.04.060

Zhao D, Xu Z, Zhang W et al (2025) Room-temperature modification of sodium lignosulfonate for enhanced phenolic hydroxyl content and its application in phenol-formaldehyde adhesives. Colloids Surf Physicochem Eng Asp 726:138121. https://doi.org/10.1016/j.colsurfa.2025.138121